CALIFORNIA INSTITUTE OF TECHNOLOGY

A Restudy of Existing Graphical Methods of Interpreting Magnetic Data and Their Application to Interpreting the Results of Magnetic Surveys Across the Los Angeles Basin

A Thesis

Submitted to the Graduate School

in Partial Fulfillment of the Requirements

for the degree

GEOPHYSICAL ENGINEER

DIVISION OF THE GEOLOGICAL SCIENCES

By

MILNER DARWIN QUIGLEY

PASADENA, CALIFORNIA

JUNE, 1949

Abstract

This thesis discusses the historical development of the methods of magnetic interpretation and explains why greater emphasis should be placed on graphical methods. Many graphical methods have been published but only one of them, Pirson's Polar Diagram method, has widespread application to all magnetic interpretive problems.

The Polar Diagram method is especially applicable to magnetic problems of a regional nature where the disturbing body is very irregular in shape and cannot be approximated by a second order geometric form. A disturbing body of this description is present in the Los Angeles Basin.

Previous attempts to match the observed magnetic anomaly curves across the Los Angeles Basin with the theoretical calculated curves by numerical methods have failed to obtain a close comparison. The Polar Diagram method makes it possible to obtain a superposition of the calculated curves over the observed curves except in the vicinity of the Palos Verde Hills. The superposition was obtained only after there was complete agreement between the existing geologic, gravity, and seismic information along the profile across the Basin.

The Polar Diagram method is one of the quickest and most straight forward of the graphical methods to use. It is applicable to most magnetic problems where the direction of the induced magnetism is parallel to the direction of the remanent magnetism.

Table of Contents

	Page
Introduction	
Statement of Problem	1
Acknowledgements	2
Methods of Magnetic Interpretation	
Historical Development	2
Discussion of Graphical Methods	4
Comparison of the Described Graphical Methods	15
Application of Different Interpretive Methonds on a Particular Problem	
Previous Work on the Los Angeles Basin	16
Application of the Two-Dimensional Polar Diagram to the Los Angeles Basin	20
Conclusions	23
Bibliography	25
Vita	27

Introduction

Statement of Problem

The question of deciding which of the four major geophysical methods of prospecting is best suited to the procurement of data on a particular geologic problem is one which always confronts the person or persons in charge of the exploration work. The final decision on this question, of necessity, will be based on the relative cost of the geophysical method, the reliability of the data obtained, and the ease, accuracy and uniqueness with which the data can be interpreted. The magnetic method unquestionably is the cheapest, the most rapid, and the easiest method with which to obtain data in the field. The difficulties are encountered in the process of the interpretation of the magnetic data. These difficulties may be traced easily to three causes. The first is that the induced magnetic field is dependent upon the angle between the strike of the disturbing body and the direction of the inducing field. Consequently, two identical structures of widely different strikes may give rise to two entirely different magnetic anomalies. The second difficulty is due to the fact that the magnetic susceptibility of rocks cannot be determined accurately. Finally, the third difficulty arises from the fact that the usual assumption of homogeneous magnetization applies only to bodies limited by surfaces of the second order (5, pg. 328-329).

The variables involved in interpreting magnetic data are so numerous that the use of magnetic methods in exploration work in the future is dependent, to a very large degree, upon the ease and assurance with

which these variables can be interpreted. Magnetic interpretation is, therefore, in need of a technique which is able to take into account all the variables so that it can be applied to most types of magnetic data with the least number of restrictions.

It is the purpose of this paper to compare the existing methods of interpretation and to select one which is most suitable for the purpose of interpreting the most general type of magnetic anomaly, i.e. the magnetic anomaly caused by an irregularly shaped geologic body of either local or regional size.

Acknowledgements

The author is very grateful to Dr. Gennady Potapenko of the Division of the Geological Sciences, who gave many invaluable suggestions and gave generously of his time in the discussion and preparation of this thesis. The author is also indebted to the other members of the staff and graduate body of the Division of Geological Sciences for helpful suggestions and criticisms. The investigation was conducted under the supervision of Dr. Potapenko in the facilities of the Division of the Geological Sciences, California Institute of Technology.

Methods of Magnetic Interpretation

Historical Development

It is of importance to review briefly the existing methods of interpretation in order to obtain a clear picture of the change of emphasis during the development of present day methods of magnetic interpretation.

The early attempts to develop interpretive procedure were centered on numerical methods. The data were obtained in the field, and then a formula was chosen which best suited the particular case. Numerical formulas were only available for the special type of geologic body which could be approximated by a buried sphere, or a cylinder, or a dike, or a semi-infinite plane. These formulas have become very numerous in the literature, but none of them is of general application and can only be applied to the data when all the restrictions are met.

During the period of the development of the numerical formulas, a few attempts were made to interpret magnetic anomalies by graphical methods. These graphical methods were in general restricted to such forms as contour maps showing lines of equal anomaly, profiles at right angles to the strike of the disturbing body, plotting of anomalous vectors, and the plotting of magnetic gradients. The latest developments in the field of magnetic interpretation have emphasized to an even greater extent the importance of graphical methods. There are several fundamental reasons why graphical methods should be given greater emphasis or consideration. In general, graphical methods are much simpler in application than numerical methods. Furthermore, graphical methods are much easier to understand by the person not especially trained in mathematics or physics. Finally and most important of all of the reasons listed, graphical methods actually represent a closer approximation to the real shape of the distrubing body, because they integrate the effect of all irregulatities and are not restricted to second order geometric figures as are numerical methods.

Discussion of Graphical Methods

Lee (7) described in 1932 a graphical method for the determination of the depth to the top of the disturbing body which causes the magnetic anomaly. Lee's method is one of construction which is based on the fact that the magnetic field due to a body decreases as a certain function of the distance from the body. Thus, by using the function $f(1/r)^n$, where r is the distance from the source, it is possible by simple construction to determine approximately the depth to the top of a buried magnetic dike, pole, or shell. Unfortuantely, this method of depth determination is restricted to those disturbing bodies which can be approximated by a dike, a pole, or a shell. Moreover, the construction method does not determine the actual shape of the body exactly. The final shape decided upon is, in an uncertain measure, a matter of extrapolation.

In 1935, Happe (3) pointed out that there were three important factors about magnetic anomalies which can be used in developing a graphical method of interpretation. The form and magnitude of any magnetic anomaly is dependent upon:

1. The dimensions and position of the disturbing body.
2. The magnetic susceptibility of the body giving rise to the anomaly.
3. The magnetizing forces present, which include the induction effects of the earth's normal magnetic field, together with any remanent magnetism of the body.

The magnitude of the anomaly is determined by all three of the foregoing factors, but the shape, form, and spatial distribution is determined by the first factor only. Thus, two bodies of the same dimensions, size, and

position relative to the places where the magnetic effects are measured will give rise to anomalies of the same form, and the anomalies will differ only in magnitude. These statements are quite true if there is no remanent magnetization present. If remanent magnetization is present, then the statements are valid only when the direction of the remanent magnetization coincides with the direction of the induced magnetization. Usually, the direction of remanent magnetization is close to the direction of the induced magnetization, so in general, it is possible to use only the relative dimensions and positions of the disturbing bodies in developing a graphical interpretation method. Happe (3, P. 218) derives formulas for the magnetic effects of an increment* of area of the disturbing body. The determination of ΔZ and ΔH can be made from the following formulas.

$$\Delta Z = K\Sigma (\cos\theta_1 - \cos\theta_2) \ln r_2/r_1$$

$$\Delta H = K\Sigma (\sin\theta_1 - \sin\theta_2) \ln r_2/r_1$$

where K is proportional to the magnetization of the body, due to its magnetic susceptibility, θ_1 and θ_2 are the angular boundaries of the increment of area, and r_1 and r_2 are the radial boundaries of the increment of area in reference to the point of measurement on the surface. Unfortunately, Happe's formulas are incorrect because:

1. He assumes in calculating the potential that the disturbing body is two dimensional in the sense that it all lies in one plane; thus the body is a thin sheet. Then Happe applies the result to a body that is a cylinder of infinite length, and hence to a body that is three dimensional and does not lie all in one plane. He considers the cross-section of the

*An increment of area is considered to be the cross section of a small prism whose length extends into infinity in the direction perpendicular to the plane of the cross-section taken through the disturbing body.

and are the vertical and the horizontal components of the Earth magnetic field respectively; and are the increments of and of caused by the disturbing body.

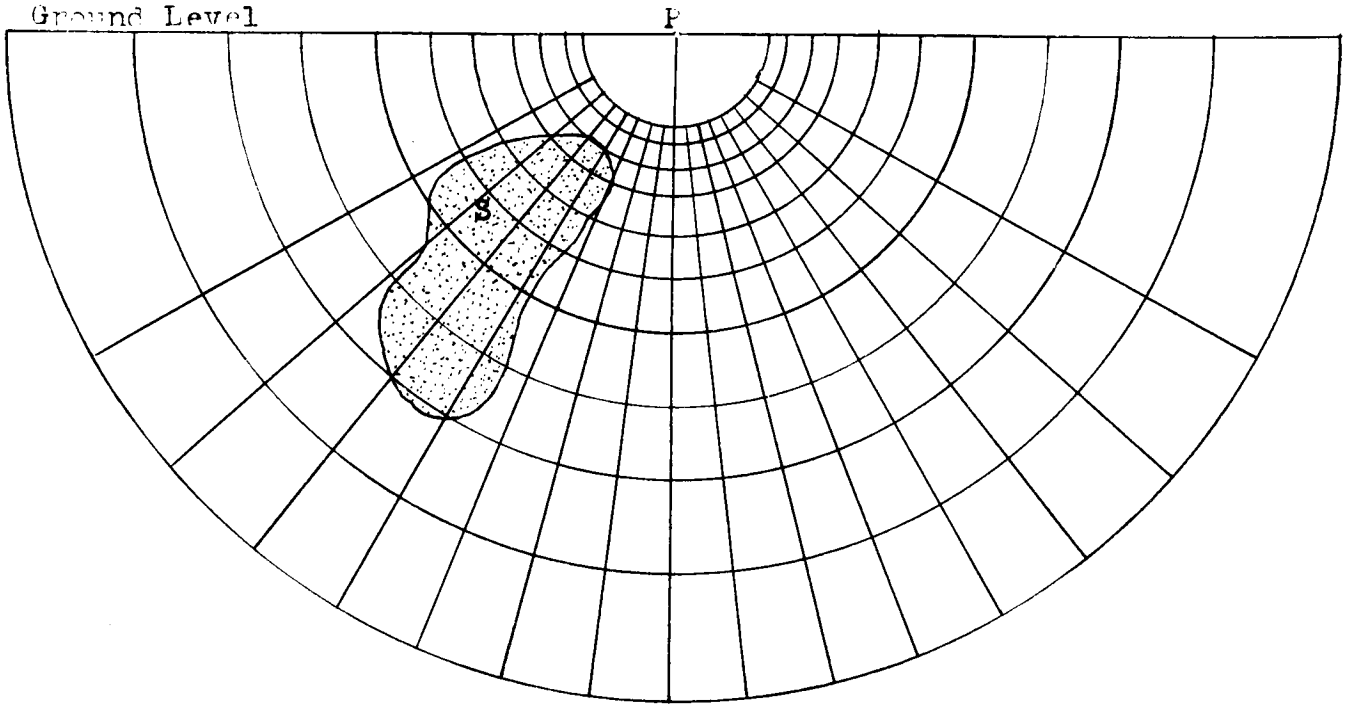

Fig. 1-- Position of graticule for calculation of Z for the point of observation P ; S is the cross-section of the disturbing body which is assumed to be infinite in the direction perpendicular to the plane of the graticule . (Copied from Hanna)

cylinder the same as that of the two-dimensional body whose potential he calculates.

2. He assumes that the effect of magnetization is to induce a density of magnetic pole strength rather than a density of dipole moment. Consequently, he does not make the necessary reference to the strike or angle of dip of the disturbing body in relation to the directions of the various components of the Earth's magnetic field.

These two errors cancel out in the r part of Happe's formulas, but not in the parts involving angles and directions.

Even though Happe's formulas are incorrect, he makes an important contribution to the field of graphical interpretation of magnetic anomalies in the manner in which he applies his formulas. He points out that the summations in the above formulas can be most easily accomplished by using a graticule as shown in Fig. 1. The graticule is constructed in such a way that Cos θ_1 - Cos θ_2 is a constant for each division. Likewise, the radii of the circles r_1, r_2, r_3, etc. are drawn so that

$$\ln r_2/r_1 = \ln r_3/r_2 = \text{Constant}$$

These constants may be chosen at will so each subdivision may be as small as desired but each subdivision will have the same effect at point P, the point of measurement. Consequently, the calculation of ΔZ at any particular point is simply reduced to counting the number of subdivisions of the graticule falling within the outline of the cross section of the disturbing body, and multiplying this number by the assigned constant magnetic effect of each subdivision at the point P. The graticule integrates the effects of all irregularities and is in no way restricted by the shape

of the cross section of the disturbing body.

The graticule shown in the diagram may be used to calculate ΔH as well as ΔZ. However, in calculating ΔH, the graticule must be rotated 90° so that the line representing the ground surface will be vertical.

When the disturbing body is not infinite in depth, then the assumption of a single polarity is no longer justifiable. The graticule will still work by passing a line through the hypothetical body at right angles to the normal direction of the magnetic dip. This line would be drawn so that the body would be more or less symmetrically divided. The upper portion could then be considered as being magnetically positive and the lower portion negative.

Happe (3, p. 219) lists five practical rules of interpretive procedure which can be listed to give a clear understanding of the use of the graticule:

1. Correct the magnetic survey data for normal and regional variations, and separate each into vertical and horizontal components.

2. Use the shape of the observed anomaly curves and all the geological information available to construct the hypothetical body.

3. Construct the cross section of the anomalous body in the plane of the magnetic meridian.

4. The anomaly due to the hypothetical body is evaluated by means of the proper graticle and the curve thus obtained is plotted to a scale suitable for comparison with the observed curve.

5. The hypothetical cross section is now modified by process of trial and error until agreement of the two curves is obtained.

Happe's graticule is very simple to use and the principle involved has widespread application to the generalized type of magnetic anomaly. Happe's particular graticule, by his own admission, has very limited utility because the cross section through the disturbing body must be taken in the plane of the magnetic meridian. This limits the use of the graticule to those bodies whose strike is nearly East - West, if the resulting problem is to be two-dimensional. This restriction is a serious limitation on the utility of the graticule, for only in the exceptional case will the strike of the disturbing body be East - West. Moreover, the incorrect nature of Happe's formulas renders the results obtained useless, even in the case of an East-West striking body.

In 1935, Bahnemann (1) published an article on the application of Nippoldt's method for determining the effect of a single pole. Nippoldt's method (9) first appeared in 1930, and since then it has been summarized by Jenny (5, p. 329), Bahnemann (1), and Heiland (4, pg. 381-389). Bahnemann extends Nippoldt's method to include the effects of a distribution of single unit poles whose combined effect approaches that of the disturbing body. The method becomes tedious for the single-pole distribution because the distribution of the poles must be varied not only in a lateral manner but in a vertical manner also. There will be numerous distributions possible that would satisfy the observed curves unless the geological control is well known. Moreover, the relation of the exact pole distribution to the actual shape of the disturbing body is unknown so that the actual shape cannot be determined by such a method.

Also in 1935, Pirson (11) described his polar diagram method. In

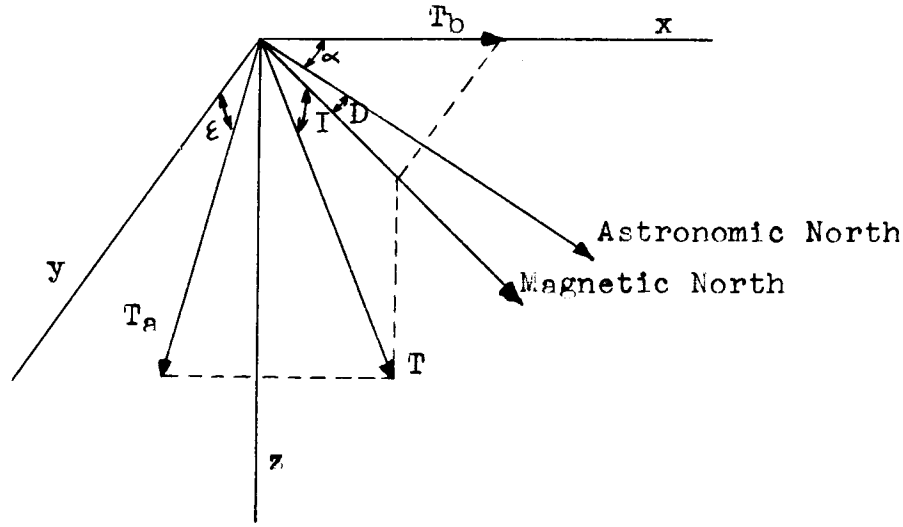

Fig. 2 - Components of the Earth's magnetic field (copied from Pirson) ∝- angle between the direction of strike of the disturbing body and astronomic North.
D - angle between astronomic North and magnetic North.
I - angle of inclination of the Earth's magnetic field.
ε - angle of inclination of the Earth's magnetic field in the direction perpendicular to the strike of the disturbing body.
T - vector representing the direction and magnitude of the Earth's total magnetic field.
T_a - vector representing the component of T in the direction perpendicular to the strike of the disturbing body.
T_b - vector representing the component of T in the direction of strike of the disturbing body.

principle, the polar diagram is very similar to the graticule suggested by Happe (3), as can be seen from the formulas given by Pirson:

$$\Delta\xi = -K\, T_a / n_e\, r_2/r_1 \left(\sin 2B_2 - \sin 2B_1 \right)$$

$$\Delta\eta = -K\, T_a / n_e\, r_2/r_1 \left(\cos 2B_2 - \cos 2B_1 \right)$$

where $\Delta\xi$ is the magnetic anomaly in the direction of T_a due to an infinite magnetic cylinder of cross section $ds = \pi (B_2 - B_1)(r_2 - r_1)$, $\Delta\eta$ is the magnetic anomaly in the direction perpendicular to T_a and due to the same cylinder, T_a is the magnitude of the component of the total Earth's field, T, in the direction perpendicular to the strike of the disturbing body, r_1 and r_2 are the radii bounding the cylinder, and B_1 and B_2 are the angles bounding the cylinder as measured from a point on the surface. The constant T_a and the double angles in Pirson's formulas arise from the fact that he takes into account the direction of magnetization in relation to the strike of the disturbing body. In essence, he corrects the invalid assumptions and omissions made by Happe. The direction and magnitude of the magnetizing vector may be calculated from the geometric relationships shown in Fig. 2. The value of T_a is given by (for notations see Fig. 2)

$$T_a = T \sqrt{\cos^2 I \, \sin^2(\alpha \pm D) + \sin^2 I}$$

It is not necessary to calculate T_b, because it does not contribute to the vertical and horizontal components of the magnetic anomalies. It is necessary, on the other hand, to calculate the value of the angle E made by the direction of T_a with the horizontal plane. This angle E can be obtained from the relationship:

$$\tan E = \tan I / \sin(\alpha \pm D)$$

Figure 3 - Polar Chart for the computation of the vertical and horizontal components of the magnetic anomaly due to a two-dimensional body, after Pirson (11). Value of each block; one gamma for $T_a = 0.5$ gauss and $k = 2000 \times 10^{-6}$ c.g.s.

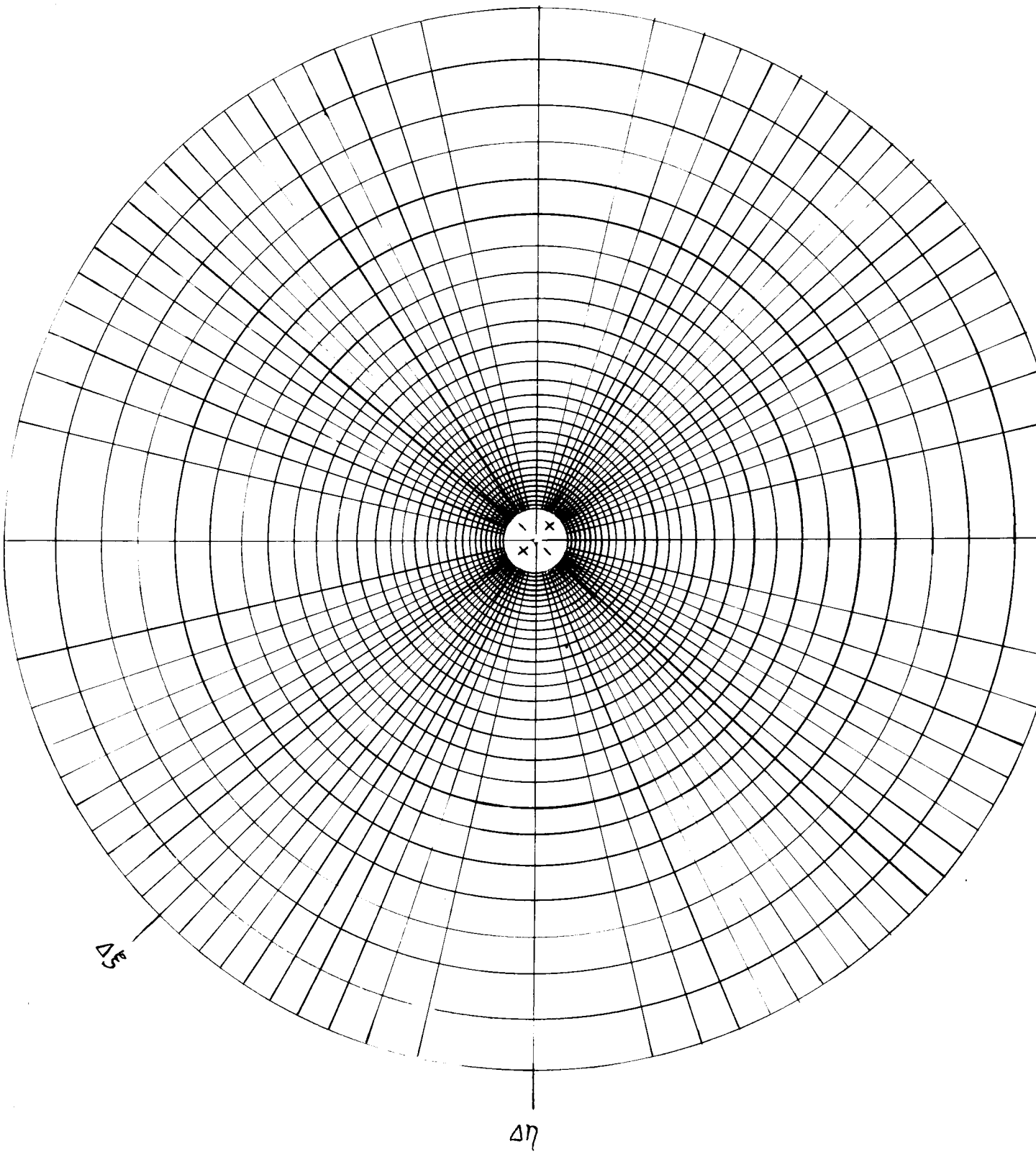
Δξ
Δη

It is possible to construct a polar diagram from the formulas for $\Delta\xi$ and $\Delta\eta$ (Fig. 3) so that each element, which represents the cross section of an infinite horizontal cylinder, produces the same effect at the center of the diagram. In the polar diagram shown, the effect of each element is one gamma when the intensity of the T_a component of the earth's magnetic field is 0.5 gauss and the magnetic susceptibility of each element is $K = 2000 \times 10^{-6}$ cgs.

If the anomalies $\Delta\xi$ and $\Delta\eta$ are known, then the vertical ΔZ and the horizontal ΔH components of the magnetic anomalies due to a subsurface geologic feature are determined by:

$$\Delta Z = \Delta\xi \sin E \pm \Delta\eta \cos E$$

$$\Delta H = \Delta\xi \cos E \pm \Delta\eta \sin E$$

where the signs $\pm$ are chosen according to the respective directions of $\Delta\xi$ and $\Delta\eta$.

It is not necessary to repeat Pirson's derivation of the formulas given, but it is important for the sake of clarity to repeat the procedure followed in obtaining the anomalies due to the assumed subsurface geologic feature.

The polar diagram (Fig. 3) is traced on transparent paper and then superimposed over a cross section of the substratum taken at right angles to the strike. The component $\Delta\xi$ is computed by laying the axis on the

polar diagram marked $\Delta\xi$ parallel to the direction of T_a, which has been drawn previously on the cross section making the angle E with the horizontal. The value of $\Delta\xi$ is simply the number of elements falling in the outline of the geologic feature, added according to their respective signs as indicated on the diagram. $\Delta\eta$ is computed in a similar manner except that the polar diagram is rotated so that the axis marked $\Delta\eta$ is parallel to the direction of T_a. If the values of T_a and $\underline{k}$ in the problem being considered do not correspond to the values given for the polar diagram, the magnetic anomalies $\Delta\xi$ and $\Delta\eta$ are obtained by proportionally reducing or increasing the computed values. The scale which is used in drawing the cross section is immaterial as long as the horizontal and vertical scales are equal. It is only necessary to select a scale such that the important part of the assumed geologic feature will be covered by the polar diagram.

The dependence of the angle of dip of T_a on the direction of strike of the geologic feature can be computed by assuming values for $\underline{I}$, $\underline{D}$, and $\underline{E}$ and then allow $\underline{E}$ to change by a prescribed amount. Thus, if $\underline{I} = 60°$, $\underline{D} = \pm 15°$, and $\underline{E} = 65°$, then from the formula,

$$\tan E = \tan I / \sin(\alpha \pm D)$$

we have

$$\tan 65° = \tan 60° / \sin(\alpha + 15°)$$

or

$$2.144 = 1.733 / \sin(\alpha + 15°)$$

therefore

$$\sin(\alpha + 15°) = 1.733 / 2.144$$

$$\alpha + 15° = \sin^{-1} .808$$

$$\alpha + 15^\circ = 54^\circ$$

$$\alpha = 39^\circ$$

Now if we change E to 60° then

$$\text{Tan } 60^\circ = \tan 60^\circ / \sin(\alpha + 15^\circ)$$

and

$$\sin(\alpha + 15^\circ) = 1$$

$$\alpha + 15^\circ = 90^\circ$$

$$\alpha = 75^\circ$$

These calculations show that a 5° change in the angle of dip of T_a corresponds to a 36° change in the strike of the disturbing body. Now, if the above values of α are used and the value of T is taken to be 0.5 gauss and k taken to be equal to 2000 x 10^{-6} cgs., then we can compute the change in the magnitude of T_a from the formula:

$$T_a = T\sqrt{\cos^2 I \sin^2(\alpha \pm D) + \sin^2 I}$$

Thus, when $\alpha = 39^\circ$

$$T_a = .5\sqrt{\cos^2 60^\circ \sin^2(39^\circ + 15^\circ) + \sin^2 60^\circ}$$

$$T_a = .5\sqrt{.25 \cdot .654 + .75}$$

$$T_a = .5\sqrt{.1635 + .75} = .5\sqrt{.914}$$

$$T_a = .5 \cdot .956 = .478$$

When $\alpha = 75^\circ$

$$T_a = .5\sqrt{\cos^2 60^\circ \sin^2(75^\circ + 15^\circ) + \sin^2 60^\circ}$$

$$T_a = .5\sqrt{.25 \cdot 1 + .75}$$

$$T_a = .5\sqrt{1.00}$$

$$T_a = .50$$

Consequently, a change of 36° in the strike of the disturbing body corresponds to a .022 change in the magnitude of T_a. Obviously, the changes

in the strike of the body and the magnitude of T_a would not be the same if different values for T, I, D, and E has been assumed. However, the computations give a general idea of sensitivity of the dip and magnitude of T_a on the strike of the assumed geologic feature.

Pirson's polar diagrams are applicable to all magnetic anomalies of the two-dimensional type. They are applicable to anomalies of regional size as well as being applicable to anomalies of local size. It is necessary that the disturbing body be much longer along its strike than it is wide in a direction perpendicular to its strike, in order to permit the two-dimensional analysis. If the disturbing body cannot be considered to be two-dimensional, then it is necessary to use a three-dimensional analysis. For this purpose, Pirson has constructed polar diagrams and depth charts for the determination of vertical anomalies due to three-dimensional bodies (11, pg. 180-185). It is not necessary to repeat the formulas and diagrams here as they will not be used in the interpretations that follow. The horizontal anomaly in the three-dimensional case is not usually computed except as a check on the computed vertical anomaly. Thus, in general, it is necessary to have only the polar charts for the computation of the vertical anomaly.

Pirson's polar diagrams present a means of obtaining a graphical solution to any anomaly arising from any conceivable shape of the disturbing body. The accuracy of the results could be expected to be very good as long as the assumption of uniform magnetization holds reasonably well. Moreover, in the case of dikes, plugs, and sills it is important to know the direction of any permanent magnetization present in

relation to the direction of the induced magnetization and the relative magnitudes of the two forces.

Jenny (5) described in 1938 a method of interpretation of magnetic data through the use of anomalous vectors. He stressed the importance of the horizontal vector in interpretation of regional anomalies over and above the use of the vertical vector. By plotting the vector triangles at the various stations the trend of the anomalous body can be determined as well as the approximate depth. His main interest was in regional anomalies where the actual shape of the disturbing body was not too critical. The use of magnetic vectors is very simple and adequate for many interpretive problems, but they are not sufficient to show the details of the actual shape of the disturbing body.

In 1945, Kogbetliantz (6) published a precise mathematical method for the quantitative interpretation of magnetic maps. Most of the final results of the procedure may be obtained from plotted curves and area determinations by a planimeter, so the method may be classified as graphical in part. The interpretation procedure is based on averaging and moment functions of the anomaly and disturbing body involved. The applications of the functions used in the interpretation necessitates their computation, and also the determination of moments with the aid of a planimeter from auxiliary curves derived from the observed anomaly curves. The functions may be tabulated to reduce the calculations in the individual case but the results give only the coordinates of the center of the disturbing body. The calculations involved seem to be much too long and time consuming to have the results so restricted. The same restriction applies

here as it does in any other mathematical procedure. The shape must be approximated by a second order geometric form. Finally, the procedure is far too involved mathematically to have widespread application.

Comparison of the Described Graphical Methods

The graphical methods which have been discussed may be placed into two classes:

1. The graphical methods which are restricted to second order forms.

2. The graphical methods which are applicable to all shapes.

The first class includes the interpretative procedures suggested by Lee, Jenny, and Mogbetliants. Each of these methods will determine only the top or center of the disturbing body - not its actual shape.

The methods suggested by Happe, Bahnemann, and Pirson belong to the second class. Happe's method was incorrect and further required that the cross section be made in the plane of the magnetic meridian. Bahnemann's method is very tedious and will only allow an approximate determination of the shape. Pirson's method is the most simple and straightforward in application of all the methods described. It has the most general application to all magnetic problems; and finally, it gives the best approximation to the actual shape of the disturbing body. For these reasons, Pirson's method was chosen in attempting to obtain a match between the observed and calculated curves across the Los Angeles Basin.

Figure 4 - Geologic Map of Los Angeles Basin showing the line of profile along which the gravitational and magnetic measurements were made after Uhrig and Schafer (13).

Reproduced from:

Gerl. Beitr. Geophys. Bd. 49

SOUTHERN CALIFORNIA

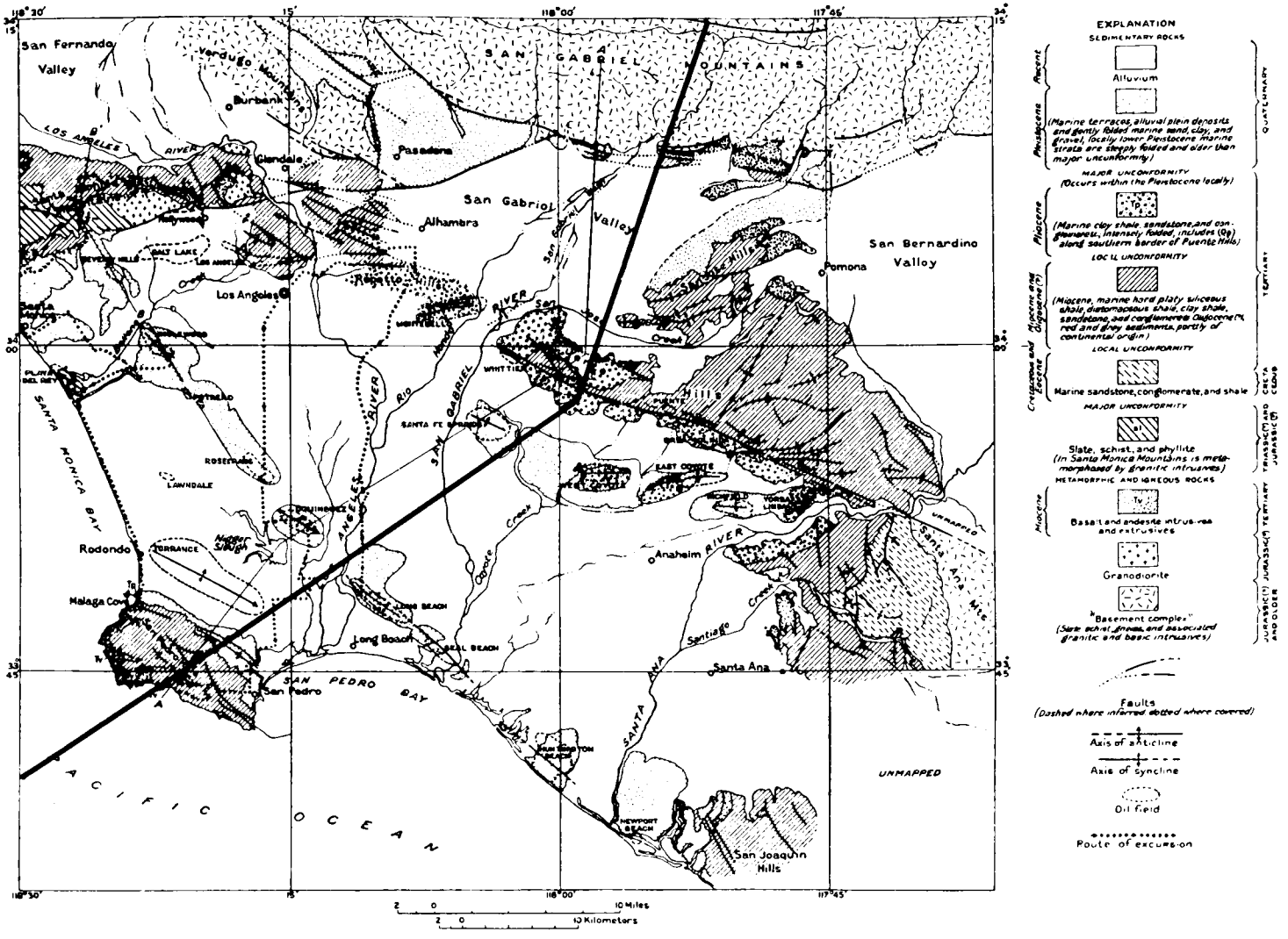

GEOLOGIC MAP OF LOS ANGELES BASIN

Compiled by H. W. Hoots and W. S. W. Kew from published and unpublished maps. Geology north of San Jose Hills from unpublished map by Rollin Eckis. For sections along lines *A–A'* and *B–B'* see Figures 1 and 2.

Figure [illegible] - Top - Gravity Profile across the Los Angeles Basin after Peterson (10). Circles represent the actual observed values corrected for elevation and topography, and the solid curve represents the theoretical curve caluclated from the hypothetical structure section.

Bottom - Hypothetical Structure section across the Los Angeles Basin and San Gabriel Mountains after Peterson (10). Assembled from geologic data and results of reflection seismograph and gravity surveys.

GRAVITY PROFILE

Computed Curve for Structure Section Shown Below

Observed Values Corrected For Elevation and Topography

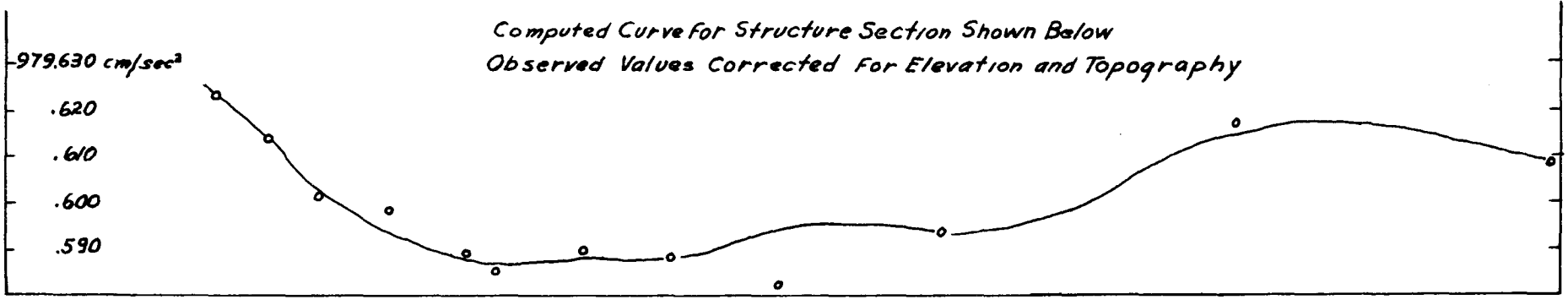

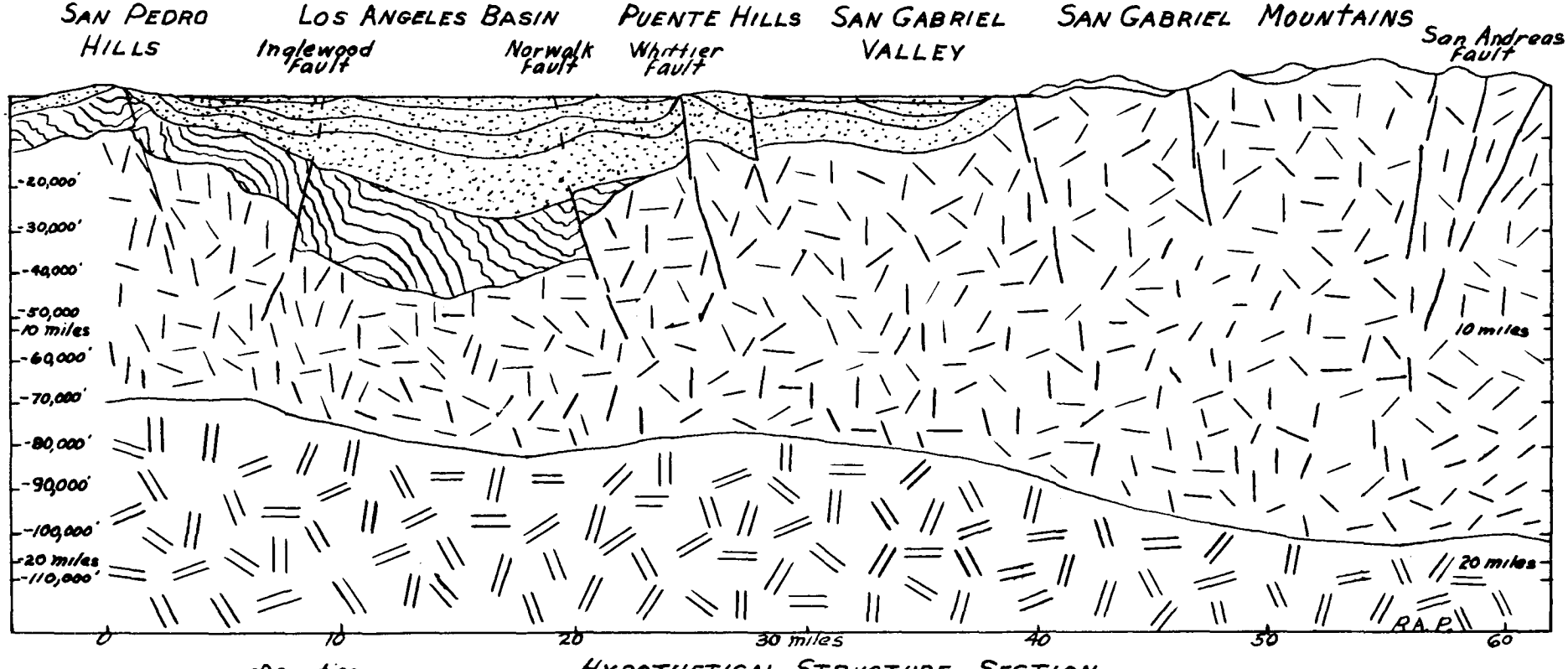

Sediments { Densities 0-10,000-2.435 gm/cc; 10-20,000-2.550 gm/cc; 20-30,000-2.600 gm/cc }

Schists, etc. Density - 2.710 gm/cc

Crystalline Rocks Density 2.710 gm/cc

Older Crystalline Rocks Density 3.110 gm/cc

HYPOTHETICAL STRUCTURE SECTION ACROSS THE LOS ANGELES BASIN AND SAN GABRIEL MOUNTAINS

Assembled from Geologic Data and Results of Reflection Seismograph and Gravity Surveys

Carved by M.D.Q.

Figure 6 - Top - Magnetic profiles across the Los Angeles Basin after Uhrig and Schafer (13). The calculated vertical and horizontal curves are based on the theoretical configuration shown on the altered hypothetical cross section.

Bottom - Altered hypothetical structure section across the Los Angeles Basin. The alterations are based on the most recent geologic data assembled from well logs, reflection seismograph and gravity surveys.

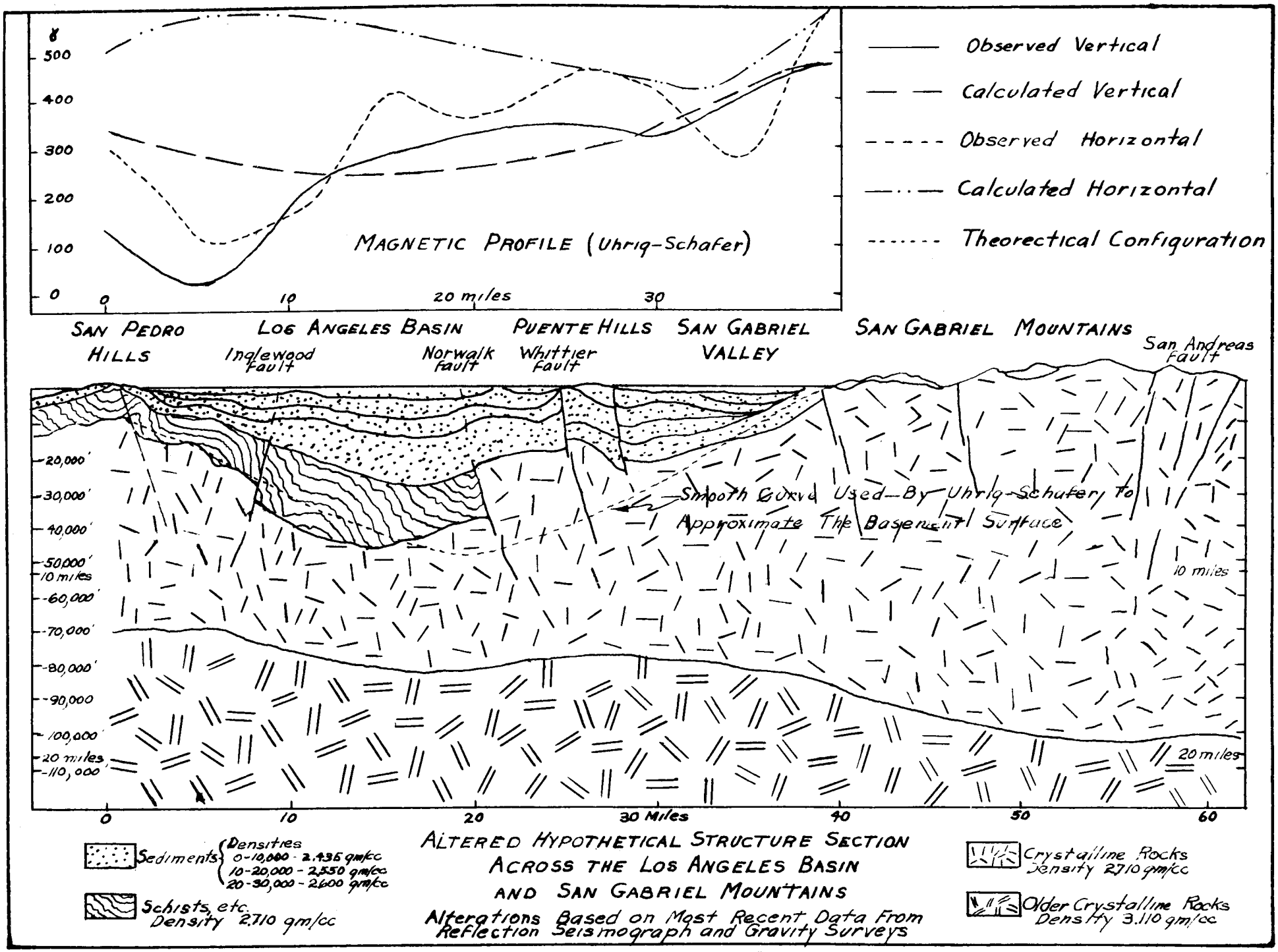
γ
500
400
300
200
100
0
0
10
20 miles
30
MAGNETIC PROFILE (Uhrig-Schafer)
Observed Vertical
Calculated Vertical
Observed Horizontal
Calculated Horizontal
Theorectical Configuration
SAN PEDRO HILLS
LOS ANGELES BASIN
PUENTE HILLS
SAN GABRIEL VALLEY
SAN GABRIEL MOUNTAINS
Inglewood fault
Norwalk fault
Whittier fault
San Andreas fault
20,000'
30,000'
40,000'
50,000'
10 miles
60,000'
70,000'
80,000'
90,000
100,000'
20 miles
110,000'
Smooth Curve Used By Uhrig-Schafer To Approximate The Basement Surface
10 miles
20 miles
0
10
20
30 Miles
40
50
60
Sediments
Densities
0-10,000 - 2.435 gm/cc
10-20,000 - 2.550 gm/cc
20-30,000 - 2.600 gm/cc
Schists, etc.
Density 2.710 gm/cc
ALTERED HYPOTHETICAL STRUCTURE SECTION
ACROSS THE LOS ANGELES BASIN
AND SAN GABRIEL MOUNTAINS
Alterations Based on Most Recent Data From
Reflection Seismograph and Gravity Surveys
Crystalline Rocks
Density 2.710 gm/cc
Older Crystalline Rocks
Density 3.110 gm/cc

Application of Different Interpretive Methods On A Particular Problem

Previous Work on the Los Angeles Basin

Uhrig and Schafer (13) measured magnetic profiles across the Los Angeles Basin in 1936. The profiles consisted of a vertical profile and a horizontal profile measured along the heavy line shown on the index map (Fig. 4). The profiles extend from the Palos Verde Hills, near San Pedro, northeastward across the Los Angeles oil field and the Puente Hills to the mouth of San Gabriel Canyon in the San Gabriel Mountains-giving a total distance of approximately 45 miles. After the profiles were obtained Uhrig and Schafer attempted to interpret the anomalies with respect to a geologic cross section across the Basin, as presented earlier by Peterson (10) in his interpretation of the gravity profile across the same basin. The cross section was based on all the geologic,seismic,and gravity information available at the time the gravity interpretation was made. This cross section is shown in Fig. 5 with the gravitational curves as measured by Peterson.

The theoretical magnetic profiles as calculated by Uhrig and Schafer (Fig. 6) are based on the mathematical process of transforming a known field about a known body into a configuration which approximates the cross section of the Los Angeles Basin. Obviously, such a method is restricted to the use of second order geometric forms such as the circle or the ellipse, and it is not sensitive to any irregularities in the cross section.

The results obtained by Uhrig and Schafer (Fig. 6) show in general a rather poor agreement between the observed and calculated anomaly curves. The transformation method is so insensitive to changes in the cross section that even a large alteration in it would not materially improve the agreement between the curves. Uhrig and Schafer suggest that the total lack of agreement in the vicinity of the Palos Verde Hills is due to inaccuracies in the cross section. This suggestion is not substantiated by more recent data. The Palos Verdes part of the cross section is proven in a measure by well data and the only change which can logically be made is to assume a basic intrusion in the vicinity instead of the quartz diorite intrusion which is shown and which is present in the rest of the basin.

There is complete agreement between the seismic data on the Palos Verde Hills area as presented by Gutenberg, and Buwalda (2) and the gravity data measured by Peterson. Moreover, there is complete agreement between the observed and calculated gravity curves in this region (Fig. 5). Consequently, any change in the cross section which permits better agreement between the observed and calculated magnetic curves must at the same time leave the seismic and gravity profiles unchanged. The only part of the cross section which does not show complete agreement between the observed and calculated gravity curves in Fig. 5 is in the vicinity of the Whittier fault. It is in this vicinity that the seismic data suggest that the top of the quartz diorite, the deep reflection horizon, could be as much as 3½ km. below the surface instead of the 1 km. shown on the cross section (Fig. 5).

Dr. J. Buwalda* stated recently that the seismic data indicate that the displacement in the basement on the Norwalk fault should be several thousand feet greater than on the Inglewood fault. Furthermore, the displacement in the basement on the Norwalk fault is much greater than it is in the overlying sediments.

The final cross section which is altered to incorporate the changes suggested above is shown in Fig. 6 with the magnetic curves obtained by Uhrig and Schafer.

The magnitude of the magnetic anomaly is determined by the magnetic susceptibility of the various formations and rocks in the geologic section chosen. On account of this fact, it is necessary to consider the magnetic susceptibility of each formation shown in Figs. 5 or 6. There is no evidence that any of the Miocene and younger formations contain any appreciable magnetizable material. It is true that they are intruded by igneous material and contain volcanic material, but most of this material, with the exception of an occasional basalt, would be considered non-magnetizable.

Uhrig and Schafer assumed the magnetic susceptibility $k = 0$ for the thick section of Franciscan schist, yet there is considerable evidence for assuming a rather high magnetic susceptibility for it. Obviously such an assumption would greatly alter the calculated magnetic profiles. Reed (12) has described the Franciscan in detail and the interesting parts of his descriptions pertaining to the susceptibility of the component parts of the Franciscan are summarized below:

1. The Franciscan conglomerate consists of a sandstone matrix and pebbles and boulders of black chert, granite, quartzite, and porphyritic

* Personal communication.

igneous rocks of different kinds including peridotites altered to serpentine and diabase.

2. The Franciscan sandstone contains magnetite in an unknown percentage.

3. The Franciscan shale contains no magnetizable material.

4. The Franciscan igneous rocks include interstratified and intrusive lavas of the basic type. Basaltic rocks occur as intrusives especially in the lower Franciscan sandstone, and as interstratified sheets of lava. Besides basalts and diabases, there are other rocks, generally serpentinized, which were originally peridotite, pyroxenite, and gabbro.

5. The Franciscan metamorphic rocks consist of quartz schist, prasinite, blue schist, talc rocks, and serpentine rocks. The prasinites are quartz free and high in albite, and like the blue schists and serpentine rocks, they may have been derived from basic igneous rocks.

Reed (12, p. 78) states that there was a great amount of igneous intrusion without much uplift and infers that a relatively large amount of the franciscan might be basic igneous rocks or derived from basic igneous material. Consequently, it seems entirely possible that parts of the Franciscan might have a $\underline{k}$ equal to more than three times the $\underline{k}$ of the underlying quartz diorite. It is doubtful that the entire Franciscan can be considered as having as high a $\underline{k}$ as suggested but when considered as a whole, it might have a susceptibility of around twice the $\underline{k}$ of the quartz diorite. The Franciscan in the center of the Basin presents two problems whose solutions may be no more than guessed. The cross sections indicate that the Franciscan schist attains a maximum thickness of about 15,000

feet in the center of the basin. It is entirely possible that not more than half of this thickness is Franciscan and the other half might be Cretaceous. Cretaceous rocks have a considerable thickness in the Santa Ana Mountains to the East, but are entirely absent on the West side of the basin. Presumably they die out to the West and may be present in considerable thickness in the center of the basin. There is no reason to believe that the Cretaceous beds, if present, contain any appreciable magnetizable material. Furthermore, there is no basis except inference for assuming that the Franciscan in the center of the Basin is intruded with considerable basic material. It is known to be intruded with basic material in the uplifted Palos Verdes area but it is not known that the intrusions carry out into the center of the Basin.

Uhrig and Schafer assumed a k equal to 900×10^{-6} cgs units for the basement on the basis that it was probably granite. However, the basement in the San Gabrial Mountains is known to be quartz diorite and therefore probably has a much higher k than Uhrig and Schafer assumed. In the final analysis, as we shall see later, the actual value of k is not critical as long as it is in the range of credibility. The relative value of k are more important, for the shape of the calculated curve is more critical than its magnitude.

Application of the Two-Dimensional Polar Diagram to the Los Angeles Basin

The ratio of the length of the Los Angeles Basin to its width is two to one. This ratio will introduce some error if we apply the two-

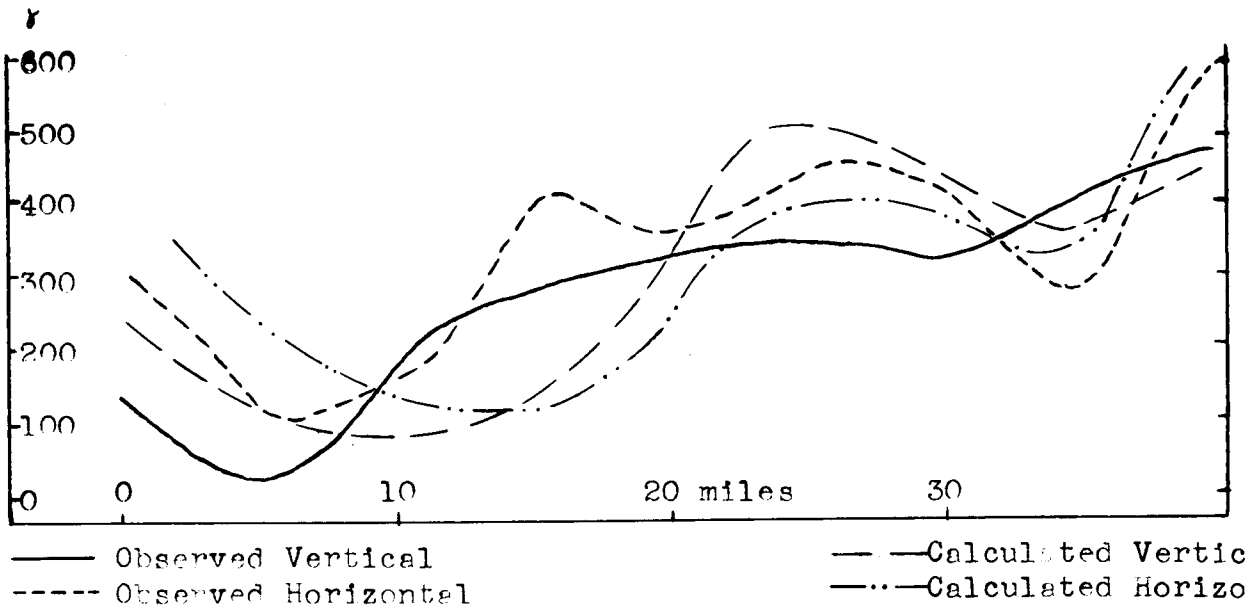

Fig. 7 Comparison of the observed and calculated magnetic profiles across the Los Angeles Basin. The calculated curves were obtained graphically by using Pirson's two-dimensional polar diagram. k(for the schist)= 0, and k(for the crystalline rocks) = 2000 X 10^{-6}c.g.s. Calculated curves are multiplied by a factor of 1.5.

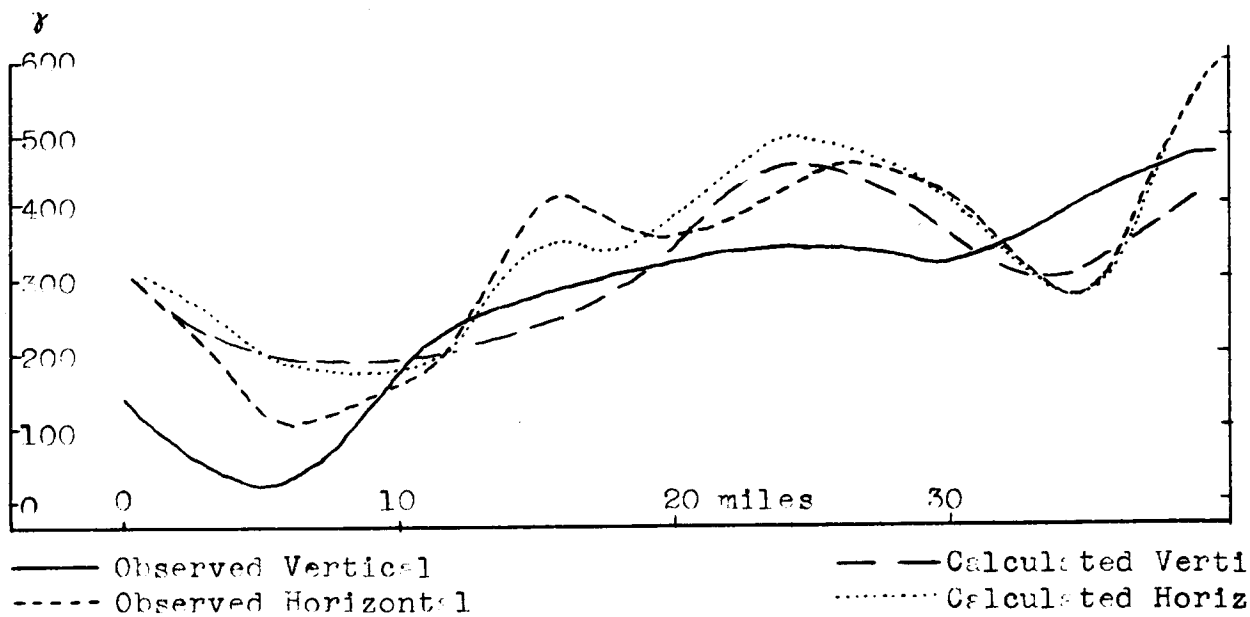

Fig. 8 Comparison of the observed and calculated magnetic profiles across the Los Angeles Basin. The calculated curves were obtained graphically by using Pirson's two-dimensional polar diagram. k(for the schist) = 4000 X 10^{-6}c.g.s., and k(for the crystalline rocks) = 2000 X 10^{-6}c.g.s. Calculated curves are multiplied by a factor of 1.5.

dimensional polar diagram in the analysis of the magnetic anomaly across the basin, but the amount of error so introduced will be relatively small, less than 10 per cent (8)*.

The polar diagram was applied first to the original cross section (Fig. 5) as drawn by Peterson and used by Uhrig and Schafer. The k for the Franciscan schists was assumed to be zero, as did Uhrig and Schafer, and the value of k for the quartz diorite and the deepest crystallines was assumed to be 2000×10^{-6} c.g.s. units. The calculated curves thus obtained are compared to the observed curves in Fig. 7. If the agreement between this set of curves is compared to the agreement obtained by Uhrig and Schafer, see Fig. 6, it will be noticed that the use of the polar diagram improves the agreement considerably. It is true that some of the peaks in the polar diagram curves depart widely from the observed curves, but an improvement in the general shape of the curves is unmistakable.

In order to improve the agreement between the observed and calculated curves further, the value of k for the Franciscan was changed from zero, to 4000×10^{-6} c.g.s. units, and the k for the quartz diorite was left at 2000×10^{-6} c.g.s. units. On applying the polar diagram, the curves shown in Fig. 8 were obtained. Now the fit between the calculated and observed curves has been greatly improved, except in the vicinity of the Palos Verde Hills and in the vicinity of the Whittier fault.

Next the polar diagram was applied to the cross section (Fig. 6) which has been altered to coincide with the latest seismic data on the basin as described earlier. The value of k for the Franciscan was assumed to be 4000×10^{-6} c.g.s. units and the k of the quartz diorite and deeper

* Nettleton's calculations refer to gravity anomalies, but due to the fact that both the gravity and the magnetic forces obey similar laws, the results are applicable to our case.

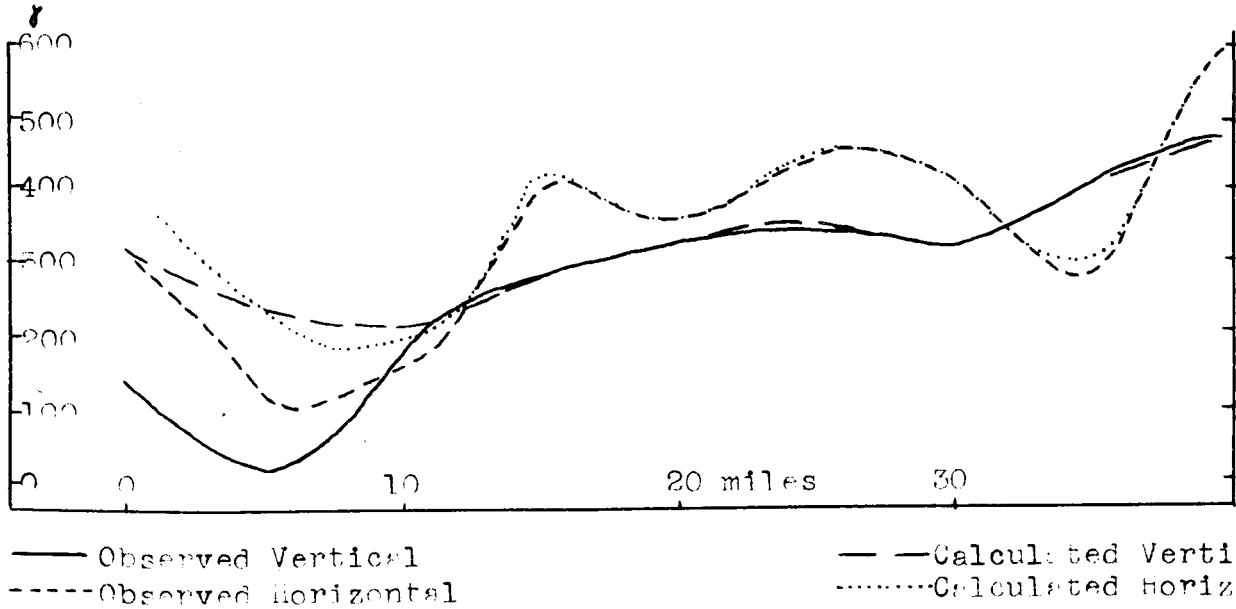

Fig. 9 Comparison of the observed and calculated magnetic profiles across the Los Angeles Basin. The calculated curves were obtained graphically by using Pirson's two-dimensional polar diagram. k(for schist) = 4000 X 10^{-6}c.g.s., and k(for the crystalline rocks) = 2000 X 10^{-6}c.g.s. Calculated curves are multiplied by a factor of 1.75.

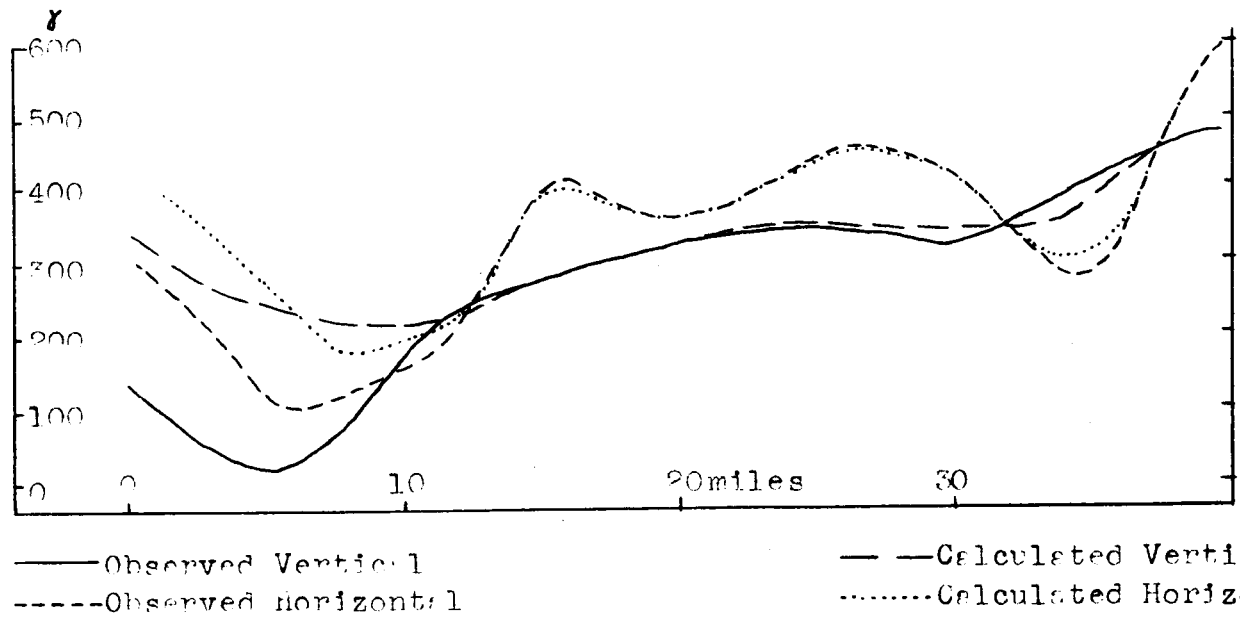

Fig. 10 Comparison of the observed and calculated magnetic profiles across the Los Angeles Basin. The calculated curves were obtained graphically by using Pirson's two-dimensional polar diagram. k(for the schist) = 4000 X 10^{-6}c.g.s., k(for the upper crystalline rocks) = 2000 X 10^{-6}c.g.s., and k(for the lower crystalline rocks) = 4000 X 10^{-6}c.g.s. Calculated curves are multiplied by a factor of 1.95.

crystallines was assumed to be 2000 x 10^{-6} cgs units. The curves obtained (Fig. 9) show almost a perfect agreement with the observed curves, except in the vicinity of the Palos Verdes Hills.

Finally the $\underline{k}$ of the deeper crystallines was changed to 4000 x 10^{-6} cgs units and the other values of $\underline{k}$ were maintained in order to determine the dependence of the fit between the observed and calculated curves on the purely hypothetical deeper crystalline horizon. The curves obtained (Fig. 10) by applying the polar diagram show almost no change from the previous set of curves. Thus it may be concluded that the lower crystalline boundary shown in the cross section does not influence noticeably the magnetic data.

The lack of agreement between the observed and the calculated curves in the vicinity of the Palos Verdes Hills can best be explained by accounting for the presence of the basic igneous rocks and their derivatives in this area. The Palos Verdes Hills represent the only uplifted area in the immediate vicinity of the profile aside from the San Gabrial Mountains. The early uplift occurred in post-Franciscan and pre-Miocene time. The absence of Cretaceous sediments in this area might well mean that the original uplift occurred in pre-Cretaceous times. During this early uplift, the Franciscan sediments were extensively intruded with basalts, peridotites, pyroxenites and other basic igneous rocks. These intrusions positively suggest a basic intrusive mass at some depth, which is probably older than the quartz diorite intrusive underlying the rest of the basin. The presence of the same basic types of rocks of the same age on the Catalina Islands makes a large basic intrusion in this region all the

more probable. Such a basic intrusion would have high magnetic susceptibility and would act as a negative magnetic mass on any magnetic profile measured Eastward from it. Consequently, both the horizontal and vertical magnetometer readings would be reduced immediately East of the Palos Verdes Hills and thereby account for the lows present in the observed curves.

The application of the two-dimensional polar diagram to the magnetic profile across the Los Angeles Basin has greatly improved the agreement between observed and calculated anomaly curves primarily because it is more susceptible to irregularities in the geologic cross section than is the method used by Uhrig and Schafer. Since the polar diagram is more susceptible to irregularities, it is more suitable to detect the irregularities or unsuspected features of the geologic cross section. The natural elimination by such a process clearly leads to a more nearly exact and unique solution of the magnetic problem. The use of the polar charts materially speeds up the calculations so that a very good fit between the observed and calculated curves is obtained in a minimum time.

Conclusions

There are a number of graphical methods which are applicable to the type of magnetic disturbing body usually found in nature, that is, the irregularly shaped body which cannot be very well approximated by a second order geometric form. It is recognized that all graphical methods are approximate and that most of them depend on the assumption of uniform magnetization. In general, however, the approximations obtained by graphical solutions are far better than the approximations

obtained by numerical formulas. The polar diagram method suggested by Pirson is one of the most straight forward and quickest of the graphical methods to use. It is applicable to most magnetic problems where the direction of the induced magnetization is parallel to the direction of the remanent magnetization. The exceptions to the coincidence of the two magnetizing forces are spectacular but relatively few in number. Some of the outstanding examples are the Kiirunavaara area, Sweden, the Kursk area, Russia, and the Pelandsberg Region, South Africa.

The two-dimensional polar diagram is sufficient in the analysis of the majority of magnetic problems. The application of the two-dimensional polar diagram to the magnetic profile across the Los Angeles Basin shows that it is satisfactory when the ratio of the length to the width of the disturbing body is as low as two to one. The polar diagram must be applied to the hypothetical geologic cross section drawn at right angles to the strike of the disturbing body. The geologic cross section must be based on all the geologic, electrical, seismic, or gravitational data available, so that the approximation to the actual cross section may be as close as possible. In the process of interpretation, this profile may be altered in steps until the desired agreement is obtained between the observed and the calculated anomaly curves. The solution of the magnetic problem thus obtained may be regarded as being a unique solution in the majority of cases, depending in a large degree on the amount of control available in drawing the first hypothetical cross section.

BIBLIOGRAPHY

1. Bahnemann, F., Graphic method for determining effects of magnetic pole distribution, A.I.M.E. Contribution 79, February, 1935; also in Trans. A.I.M.E., Geophysics, vol. 138, pg. 165-172, 1940.
2. Gutenberg, Beno., and Buwalda, J. P., Seismic reflection profile across the Los Angeles Basin, Proc. Geol. Soc. Amer. 1935, pp. 327-328.
3. Happe, Bernard, Magnetometric surveying, Mining Magazine, vol. 53, pg. 217-219, 1935.
4. Heiland, C. A., Geophysical Exploration, Prentice-, Hall Inc., New York, pg. 381-389, 1940.
5. Jenny, W. P., Magnetic methods, Science of Petroleum, vol. 1, pg. 328-345, 1938.
6. Kogbetliantz, E. G., Quantitative interpretation of maps of magnetic and gravitational anomalies by mathematical methods, Quarterly of Applied Mathematics, vol. 3, pg. 55-75, April, 1945.
7. Lee, F. W., Results of some magnetic measurements on dikes, with experiments upon geophysical differentiation of nickel-ore deposits in the Sudbury District, Ontario, Canada, U.S. Bur. of Mines, Tech. Paper 510, 1932.
8. Nettleton, L. L., Geophysical Prospecting for Oil, McGraw-Hill Book co., New York, p. 117, 1940.
9. Nippoldt, A., Verwertung Magnetischer Messungen zur Mutung Fuer Geologen und Bergingenieure; Verlag von Julius Springer, 74 pages, 1930.

10. Peterson, R. A., Results of Gravity Measurements in Southern California, Unpublished Doctor's Thesis, 1935, Calif. Inst. of Tech., Pasadena 4, Calif.

11. Pirson, Sylvain J., Polar charts for interpreting magnetic anomalies, A.I.M.E. Contribution 91, November 1935; also in Trans. A.I.M.E., Geophysics, vol. 138, pg. 173-185, 1940.

12. Reed, Ralph D., Geology of California, published by A.A.R.G., pg. 77-97, 1933.

13. Uhrig, L. F., and Schafer, Sidney, observed and calculated values of the magnetic intensity over a major geologic structure, Masters Thesis, 1937, Calif. Inst. of Tech., Pasadena 4, California; also in, Balch Graduate School of the Geological Sciences, Calif. Inst. of Tech. Contribution No. 205; Reprinted from, Gerlands Beitraege zur Geophysik, vol. 49, pg. 129-139, Feb., 1937.

VITA

Date of Birth:	July 28, 1918
Academic Career:	Quincy High School, Quincy, Michigan, 1931-1935.
	Michigan State College, East Lansing, Michigan, 1937-1941.
	Northwestern University, Evanston, Illinois, 1941-42, 1946-47.
	California Institute of Technology, Pasadena, California, 1947-1948.
Degrees received:	Bachelor of Science, Michigan State College, 1941
	Master of Science, Northwestern University, 1947.
Positions held:	Junior Geologist, Michigan State Geological Survey, Lansing Michigan, 1940-1941.
	Geologist, Magnolia Petroleum Company, Mattoon, Illinois. Summer of 1941.
	Assistant in Geology, Department of Geology, Northwestern University, 1941-42.
	Physicist, P3, U.S. Naval Bureau of Ordnance, Washington, D. C., 1942-45.
	Assistant in Geology, Department of Geology, Northwestern University, 1946-1947.
	Geologist, Sinclair Wyoming Oil Co., Salt Lake City, Utah, Summer of 1947.
	Instructor in Geology, Division of the Geological Sciences, California Institute of Technology, 1947-1948.
	Geologist, Sinclair Wyoming Oil Co., Salt Lake City, Utah, June 1948-